cation—a two-dimensional scan of a piece of sphalerite (ZnS) containing inclusions of iron pyrites (sulfides of iron). An *XY* stage driven by a stepping motor moved the sample in a raster pattern past the stationary pinhole. The iron picture (Fig. 3b) and zinc picture (Fig. 3c) account for most of the specimen, but occasional dark spots in *both* aroused our curiosity; spectra at those points identified two different kinds of "blebs," one rich in calcium (Fig. 3d) and the other rich in silicon (Fig. 3e). These pictures were taken in air, which has the additional advantages of preventing sample charging, owing to the ionized discharge path along the proton beam, as well as of allowing cooling of the sample by convection from the surface. [Air has the disadvantage of showing a strong argon line, and, at a much lower level, a krypton line (1.1 ppm in air). The ability to see these natural constituents gives some idea of the sensitivity of this technique. A helium environment eliminates these lines, of course, and, in addition, reduces multiple scattering and attenuation.]

The results so far have been obtained with a crude experimental arrangement—a low beam current (1 to 100 pa), large pinholes, and a small detector. Some idea of the improvement possible with smaller pinholes is shown in Fig. 4, the sphalerite specimen at higher magnification. The smaller pinhole (25 μm in diameter) yields considerably better resolution, at the expense of signal. By using a smaller pinhole, some electromagnetic prefocusing, higher beam intensities, along with computerized data-taking and the techniques of image enhancement, we expect to improve the microscope's capabilities, reaching a resolution of $\lesssim 1$ μm.

Owing to its properties of (i) operation in an atmospheric environment, (ii) relatively high penetrating power, and (iii) chemical element discrimination, even of adjacent elements in the periodic table at extremely low concentrations, the scanning proton microprobe would appear to have applications in many disciplines but most particularly in the biological sciences. Microscopy of hydrated or even live specimens is possible; alternatively, the specimen could be frozen or maintained in an atmosphere saturated with water vapor to prevent drying of thin specimens during exposure. Very little preparation is needed—it is not necessary to stain the specimen or to produce thin sections—and, because of the good penetration, with consequent large depth of field, it is possible to make in-focus micrographs of the same object viewed at two angles, with subsequent stereoscopic interpretation. The range of possible applications, several of which are now being pursued, includes environmental studies (distribution of contaminants in microorganisms); human biochemical assays (for example, in hair) in subjects both living and dead (mummies); solid-state studies (junctions, microcrystals, and the like); cell biology; and metallurgy. The availability of about 100 proton accelerators in this country alone, capable of producing 2- to 4-Mev beams of sufficient intensity ($\gtrsim 10$ μa/mm^2), should make this extremely simple technique attractive for research in a variety of disciplines.

P. HOROWITZ

Department of Physics, Harvard University,
Cambridge, Massachusetts 02138

L. GRODZINS

Department of Physics, Massachusetts
Institute of Technology, Cambridge 02139

References and Notes

1. F. S. Goulding and J. M. Jaklevic, *Annu. Rev. Nucl. Sci.* **23**, 45 (1973).
2. T. B. Johansson, R. Akselsson, S. A. E. Johansson, *Nucl. Instrum. Methods* **84**, 141 (1970).
3. R. G. Flocchini, P. J. Feeney, R. J. Sommerville, T. A. Cahill, *ibid.* **100**, 397 (1972).
4. F. Folkmann, C. Gaarde, T. Huus, K. Kemp, *ibid.* **119**, 117 (1974).
5. J. A. Howell, thesis, Harvard University (1974). Much better sensitivity (parts per million) for the detection of trace elements can be obtained by detecting fluorescence induced by *monochromatic* x-ray irradiation (*1*); however, this is not relevant to microprobe analysis, since counting rates are impractically small for finely collimated monochromatic x-ray beams.
6. V. E. Cosslett and P. Duncomb, *Nature (Lond.)* **177**, 1172 (1956).
7. J. V. P. Long and V. E. Cosslett, *X-ray Microscopy and Microradiography* (Academic Press, New York, 1957).
8. P. Horowitz and J. A. Howell, *Science* **178**, 608 (1972).
9. J. A. Cookson, A. T. G. Ferguson, F. D. Pilling, *J. Radioanal. Chem.* **12**, 39 (1972).
10. For instance, 1 na of 2-Mev protons incident on a carbon matrix (1 mg/cm^2) containing 1 part in 10^4 by weight of a trace element produces count rates (in counts per second) of 3×10^3, 6×10^2, 1.5×10^2, 9×10^2, and 7.5×10^2 for trace elements of atomic number 12 (magnesium), 20 (calcium), 30 (zinc), 40 (zirconium), and 50 (tin), respectively, assuming a detector subtending $0.1 \times 4\pi$ steradian.
11. For instance, multiple scattering of the collimated proton beam in air, from pinhole to sample, broadens the beam by about 0.2 μm for 2-Mev protons over a path length of 0.1 mm; for a path length of 1 mm the broadening is 5.8 μm. The corresponding figures for a helium path are 0.04 and 1.4 μm. Multiple scattering in the target sample broadens a 2-Mev proton beam by 0.18 μm for a 1 mg/cm^2 carbon sample of unit density (10 μm in thickness); for a 10 mg/cm^2 sample (100 μm in thickness) the corresponding figure is 5.8 μm.

12. We thank J. Ryan and H. Rosen (Lincoln Laboratory, Massachusetts Institute of Technology) for their proton beam and laboratory support, W. Ladd and A. Eisenman for assistance in construction and data-taking, M. Bottino (Brooklyn College) who provided the sphalerite sample, and T. Clarkson (University of Rochester) who provided the hair sample. This work was supported with funds from the Alfred P. Sloan Foundation, the National Science Foundation (grant DMA 74-23522), and the Atomic Energy Commission [contract At(11-1)-3069].

13 May 1975

Hydroxyl Radical Concentrations Measured in Ambient Air

Abstract. *Diurnal variations in the hydroxyl radical concentration of ambient air were measured for the first time by the technique of laser-induced fluorescence.*

It has been suggested in recent years that the hydroxyl radical (HO) is a major driving force in the chemistry of the atmosphere. It sustains photochemical chain reactions which determine the chemical transformation of numerous trace constituents of urban (*1*) and natural atmospheres (*2*). A measurement of the HO concentration in the atmosphere could provide a vital new insight into the understanding of photochemical smog as well as a better quantitative basis for the assessment of the impact of man-made chemical emissions on a global scale.

The HO concentration has been estimated from considerations of the global balance of CO (*3*) and from photochemical considerations of reactions operative in the troposphere (*4*). It has been measured in the stratosphere by observing the fluorescence of HO excited by the solar radiation (*5*). However, this technique cannot be used for HO measurements at lower altitudes because of the reduced fluorescence efficiency and the multitude of interferences present there. Very recently, a measurement of HO concentration at ground level has been made by means of laser-induced fluorescence (*6*). We report here on the HO concentration in the open air measured by means of this technique.

Detection scheme. The technique of laser-induced fluorescence for HO measurements involves the excitation of HO radicals from the ground electronic state to the first excited electronic state and the detection of the resulting fluorescence emitted by the excited HO. At ambient temperatures, most of the population resides in the lowest two rotational levels of the ground state. The excitation used in this work was the $P_1(2)$ line near 2825.8 Å in the $^2\Pi(\nu = 0) \rightarrow {}^2\Sigma^+(\nu = 1)$ transitions (*7, 8*) of HO. The excited HO undergoes very fast relaxation under atmospheric conditions, finds its way into the $^2\Sigma^+(\nu = 0)$ manifold, and then fluoresces in the $^2\Sigma^+(\nu = 0) \rightarrow {}^2\Pi(\nu = 0)$ transitions (*6, 8*). This fluorescence is centered around 3090 Å, with a spectral width of about 30 Å. The HO concentration is then deduced from the fluorescence measurements by the use of Eq. 1:

$$n = S(A\sigma_a\eta_F)^{-1} \qquad (1)$$

Here n represents the HO concentration in the focal region of excitation; S is the fluorescence signal; A is a measure of the intensity of excitation and the detection efficiency for the particular arrangement em-

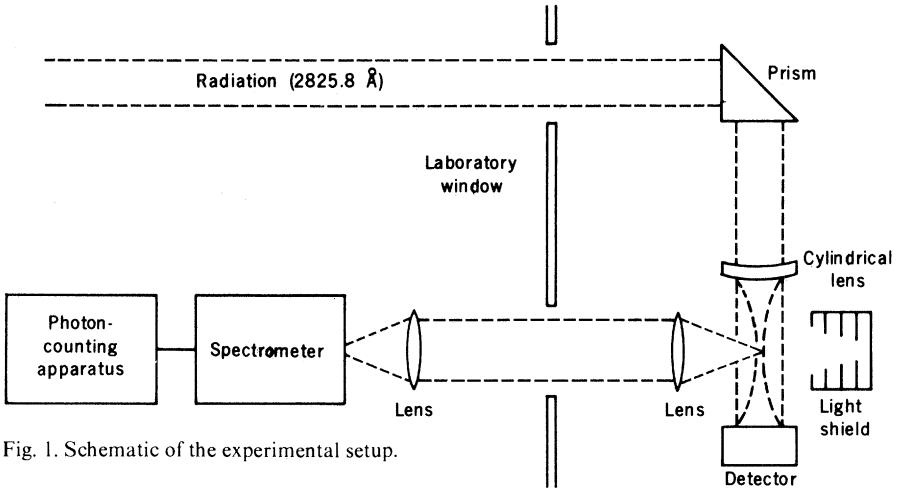

Fig. 1. Schematic of the experimental setup.

ployed in the experiments; σ_a is the absorption cross section of HO for the particular transition used for excitation; and η_F is the fluorescence efficiency.

For the results reported here, A was determined by comparing the HO fluorescence with the spontaneous Raman scattering of molecular nitrogen near 3025 Å; $\sigma_a = 2 \times 10^{-17}$ cm^2 for the $P_1(2)$ transition for a room-temperature distribution; and η_F is estimated to be 0.01. From the estimated uncertainties in these parameters, the uncertainty in the HO concentration deduced according to Eq. 1 is about a factor of 3 (*6*).

An independent calibration of the laser technique has been made by means of experiments in a smog reactor, in which the HO concentration was simultaneously measured by laser-induced fluorescence and estimated by a chemical method (*9*). The results from these two independent methods are in good agreement within the absolute uncertainty of the two methods. Details of these experiments will be published elsewhere (*10*).

As has been indicated, the experiments were carried out with a laser source of wavelength tunable near the $P_1(2)$ line (2825.8 Å) of HO. This light was obtained as the second harmonic of the output from a dye laser system; this laser system consisted of an oscillator coupled with an amplifier, and was operated with purified rhodamine 6G dissolved in methanol and at a repetition rate of one pulse every 12 seconds. We narrowed the spectral width of the output by using a Littrow grating as an end reflector and an intracavity Fabry-Perot etalon. We did the fine tuning by varying a mixture of helium and propylene, which filled the etalon spacing. The output pulse from the laser typically measured 20 mj in energy and 0.2 cm^{-1} in spectral width, and lasted about 0.3 μsec. The second harmonic of the output was generated in a 5-cm crystal of ammonium dihydrogen phosphate oriented for index matching. The output energy of the second harmonic light was about 0.2 mj or less.

Figure 1 depicts the experimental setup for the HO fluorescence measurements. The second harmonic beam near 2825.8 Å was focused with a cylindrical lens to a strip 1 mm by 5 mm in the open atmosphere about 60 cm outside our laboratory window and about 3 m above the ground. The window overlooks a grass lawn and faces south. The light scattered in a direction 90° from the exciting radiation was collected with $f/3$ optics and was processed through two spectrometers (Spex model 1700) operated in tandem. The rejection ratio measured with this arrangement was 1 part in 10^4 at 25 Å away from the spectrometer setting, and less than 1 part in 10^7 at 100 Å or more away. The output from the spectrometers was then detected by a high-gain photomultiplier and related photon-counting apparatus.

We tuned the exciting radiation to coincide with the $P_1(2)$ transition of HO by observing the enhanced fluorescence near 3090 Å resulting from excitation of the high concentrations of HO in a gas burner flame. The background (off-resonance) signal was taken as the fluorescence yield near 3090 Å in ambient air when the excitation was detuned 5 cm^{-1} from the $P_1(2)$ transition. The on-resonance and off-resonance measurements were made alternately, and the difference in the two signal levels was taken as the fluorescence yield due to the ambient HO.

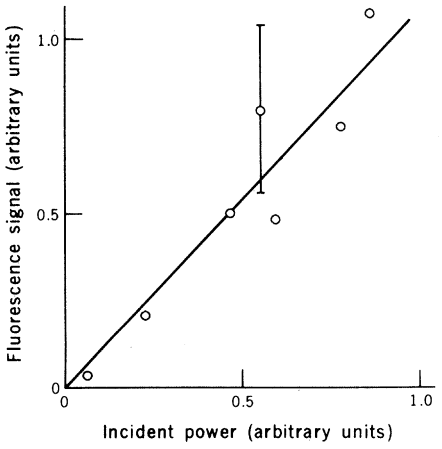

Fig. 2. Power dependence of the observed fluorescence signal near 3090 Å. By partially shielding the focal region with a box measuring 2 by 1 by 1 m, we were able to reduce the O_3 concentration near the focal region to about 2 ppb without affecting the HO concentration. Under this arrangement, O_3 interference contributes negligibly to the observed HO signal. This shielding was used for this power dependence measurement only.

Early experiments conducted with a tightly focused beam showed that care must be taken to minimize interferences due to two-photon dissociation of water (*11*) and laser-induced dissociation of ambient O_3 (*12*), which lead to HO formation. It was for this reason that a large focal strip and reduced energy per pulse were used for excitation. With these improved arrangements, we have observed (Fig. 2) that the fluorescence signal is approximately linearly dependent on the power of the exciting radiation. This linear dependence indicates that the observed fluorescence is due to the ambient HO rather than to HO generated by the laser radiation.

Ancillary measurements of other atmospheric trace constituents were made near the focal region of excitation to examine chemical relations between HO and these species. These include CO, CO_2, NO, NO_2, CH_4, and nonmethane hydrocarbons (*13*).

Detection limit. The background count due to the dark current of our photon-counting apparatus was less than one photoelectron per 1000 laser shots, and the background due to internal scattering inside the spectrometers was less than one event per 100 laser shots in the region of the HO fluorescence. These background counts are relatively unimportant in determining the detection limit with our present experimental capabilities (*6*).

With off-resonance excitation, the fluorescence yield near 3090 Å was found to be essentially constant within the statistical uncertainty both throughout the course of a day and from one day to the next. The statistical uncertainty is associated with the random arrival of single photoelectric events. The observed off-resonance fluorescence is at a level of about one event per 10 laser shots and corresponds, according to the calibration factor of Eq. 1, to an HO concentration of 3×10^7 molecule cm^{-3}. The source of this off-resonance fluorescence remains unknown, however.

At present, our detection limit is determined by this off-resonance fluorescence near 3090 Å and by our ability to read into the statistical uncertainty associated with this background fluorescence. Our present HO detection limit is about 5×10^6 molecule cm^{-3}.

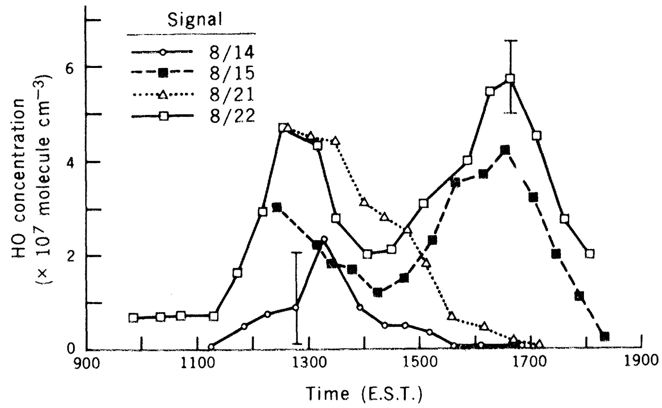

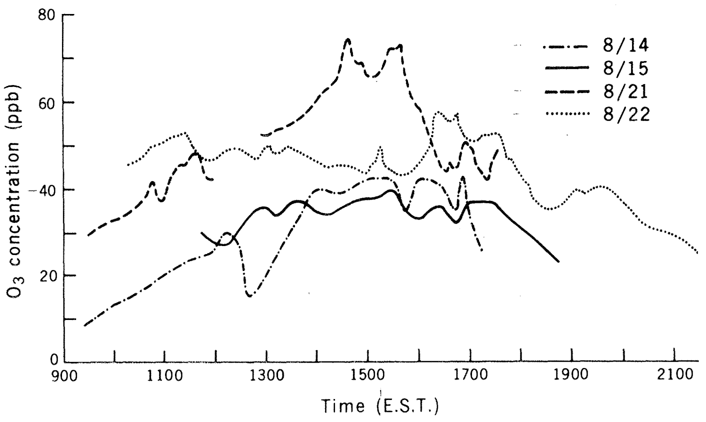

Fig. 3 (left). Diurnal variation of the HO concentration for 4 days in 1974. Each data point represents an average of 100 laser shots over a period of about an hour. The error bar indicates the statistical uncertainty associated with each data point, becoming larger as the signal level is lower. Fig. 4 (right). Diurnal variations in the O_3 concentration concurrent with the HO concentration shown in Fig. 3.

Atmospheric measurements. Measurements of HO concentrations in the open air were conducted through the months of June, July, and August 1974. Diurnal variations were observed for several consecutive sunny days in August (Fig. 3), when the HO concentration reached the highest value observed. This may be contrasted with the results on rainy or cloudy days when the HO concentration was below the detection limits of 5×10^6 molecule cm^{-3}. In Fig. 3, the HO concentration is seen to build up during the late morning hours, reach a peak in the afternoon, and drop back to below the background (off-resonance) signal in the afternoon. Occasionally, a second peak of comparable height occurred later in the afternoon.

The HO concentrations presented in Fig. 3 represent running averages over 100 or more laser shots. The absolute values for these deduced HO concentrations may be uncertain by as much as a factor of 3 because of the uncertainty in the fluorescence efficiency of the excited OH discussed above.

The results in Fig. 3 have been corrected for the interference effect due to the laser-induced dissociation of O_3 (*12*). With the measured ambient O_3 concentration, this correction typically amounted to an equivalent HO concentration of about 1×10^7 molecule cm^{-3}. No corrections were made for other interference effects such as the laser-induced dissociation of nitrous acid (*14*) (HONO). Experiments carried out in a smog reactor indicate that, at the exciting intensity used for outside measurements, as much as 0.5×10^6 molecules per cubic centimeter of HO can be generated per 1 part per billion (ppb) of HONO. With an estimated ambient HONO concentration of 1 to 10 ppb, it is thus possible that the true HO concentration in the ambient air is somewhat lower than that depicted in Fig. 3.

Concurrent observations of several atmospheric trace constituents revealed no apparent correlation with the HO concentration. For instance, continuous records of the O_3 concentration shown in Fig. 4 do not exhibit any distinct diurnal pattern. Although it is generally higher in mid-afternoon, there is no appreciable decrease in the O_3 concentration at night. The observed average O_3 concentration of about 40 ppb is comparable to the natural background level (*15*). The concentrations of CO, NO, and NO_2 varied more or less randomly throughout the entire monitoring period by as much as 50 percent from their mean values of 0.5 part per million (ppm), 3 ppb, and 20 ppb, respectively. Although the NO concentration is near the natural background level (*2, 16*), both CO and NO_2 are much higher than their corresponding natural background concentrations (*13, 16, 17*) of 0.14 ppm and 2 ppb. The CH_4 concentration remains steady at the natural background level (*18*) of 1.55 ± 0.05 ppm at all times. Numerous nonmethane hydrocarbons were observed at concentrations below the 10 ppb level (by volume), but detailed analyses were not carried out. The relative humidity was about 50 percent at a typical daytime temperature of 27°C.

Implications to atmospheric chemistry. The results presented in Fig. 3 indicate that (i) the HO concentration in the ambient air can exceed 10^7 molecule cm^{-3} and (ii) the HO diurnal variation shows a peak in the early afternoon and occasionally exhibits a second peak in the late afternoon. The observed peak values are, at first glance, consistent with earlier estimates based on the photochemistry of the natural troposphere in the summertime (*2, 4, 5*). In order to correlate this value with the yearly daytime average HO concentration derived by Weinstock (*14*), 5×10^6 molecule cm^{-3}, a knowledge of the seasonal variation in the HO concentration is needed. On the basis of estimates from the photochemical model (*2*), the average value is about half that of the summertime value. One-half of 10^7 molecule cm^{-3} gives an average daytime value of 5×10^6 molecule cm^{-3}, which is in good agreement with Weinstock's value. However, the occurrence of a second peak in the HO concentration is not predicted in the model calculations for the natural troposphere. As indicated earlier, the results of the ancillary chemical measurements also show that the concentrations of a number of atmospheric constituents deviate from those used in these model calculations. The chemical implications of these observations warrant brief discussion here, although an extensive discussion of atmospheric chemistry is beyond the scope of this report.

The relevant feature of the photochemistry of the natural troposphere is the occurrence of a cyclic chain relationship between HO and HO_2 radicals, involving reactions with CO, CH_4, NO, and other species. Under conditions of the natural troposphere, that is, all species present at their natural background concentrations, these reactions sustain a long chain reaction in which HO is produced primarily from HO_2 through reaction with NO, and HO is removed by reaction with CO and CH_4 with subsequent regeneration (*19*) of HO_2. This source of HO production is highly efficient and is more important than direct photochemical production (*20*) of HO. In this case, the HO concentration is expected to correlate with the concentrations of these reacting species, and the diurnal variation of the HO concentration should show a single peak early in the afternoon.

The concurrent ancillary chemical data show that both CO and NO_2 concentrations were significantly above their natural background levels whereas the CH_4, CO_2, NO, and O_3 concentrations were close to their background levels. The presence of higher concentrations of CO and NO_2 will markedly affect the efficiency of the HO chain reaction; that is, they will shorten the HO reaction chain and will lower the predicted HO concentration relative to that for the natural troposphere (*21*). Therefore, the observation of a peak HO concentration greater than 10^7 molecule cm^{-3} would suggest the presence of an efficient, direct photochemical source of HO. A plausible mechanism involves HONO (*22*), which generates HO upon dissociation by the solar radiation. The importance of this reaction in smog formation (*23*) has been recognized for some time. Estimates based on the absorption cross section of HONO indicate that concentrations in the parts-per-billion range would lead to the generation of excess HO concentrations, sufficiently high to explain the enhanced peak values observed here, and may also explain the occurrence of a second HO peak in the late afternoon. Work is in progress to ascertain the relevance of this mechanism.

To summarize, diurnal variations in the HO concentration of ambient air were measured for the first time by the technique of laser-induced fluorescence. The HO concentration builds up in the morning, peaks in the afternoon, and decreases to below the detection limit at night. The peak HO concentration also varies from day to day; it reaches a level in excess of 10^7 molecule cm^{-3} on sunny summer days but is below the detection limit on rainy or cloudy days. Our results indicate that, in addition to processes operative in the natural troposphere that produce HO, direct production of HO through photodissociation of atmospheric contaminants such as HONO may also play an important role in determining the HO concentration observed in our measurements.

CHARLES C. WANG, L. I. DAVIS, JR.
C. H. WU, S. JAPAR
H. NIKI, B. WEINSTOCK
Scientific Research Staff, Ford Motor Company, Dearborn, Michigan 48121

References and Notes

1. H. Niki, E. E. Daby, B. Weinstock, *Adv. Chem. Ser.* **113**, 16 (1972); K. L. Demerjian, J. A. Kerr, J. G. Calvert, *Adv. Environ. Sci. Technol.* **4**, 1 (1974).
2. H. Levy, *Adv. Photochem.* **9**, 369 (1974).
3. B. Weinstock and H. Niki, *Science* **176**, 290 (1972); B. Weinstock and T. Y. Chang, *Tellus* **26**, 108 (1974).

H. Levy II, *Science* **173**, 141 (1971); J. C. McConnell, M. B. McElroy, S. G. Wofsy, *Nature (Lond.)* **233**, 187 (1971).

5. J. G. Anderson, *J. Geophys. Res.* **76**, 7820 (1971).
6. C. C. Wang, *Bull. Am. Phys. Soc.* **19**, 24 (1974); ______ and L. I. Davis, Jr., *Phys. Rev. Lett.* **32**, 349 (1974); E. L. Baardsen and R. W. Terhune, *Appl. Phys. Lett.* **21**, 209 (1972).
7. G. H. Dieke and H. M. Crosswhite, *J. Quant. Spectrosc. Radiat. Transfer* **2**, 97 (1961).
8. C. C. Wang and L. I. Davis, Jr., *Appl. Phys. Lett.* **25**, 34 (1974).
9. The chemical determination of the HO concentration involves measuring hydrocarbon decay rates in the photolysis of mixtures of NO_x ($NO + NO_2$) and hydrocarbons (in the parts-per-million concentration range) in a smog reactor. The HO concentration can be determined from these measurements and the known rate constants for hydrocarbon-HO reactions.
10. C. H. Wu, S. Japar, H. Niki, C. C. Wang, L. I. Davis, Jr., in preparation.
11. C. C. Wang and L. I. Davis, Jr., *J. Chem. Phys.* **62**, 53 (1975).
12. ______, C. H. Wu, S. Japar, in preparation.
13. Nonmethane hydrocarbons, CO_2, CO, and CH_4 were monitored by conventional gas chromatographic techniques with flame ionization detection [M. B. Colket, D. W. Naegeli, F. L. Dryer, I. Glassman, *Environ. Sci. Technol.* **8**, 43 (1974); A. P. Altshuller, *Adv. Chromatogr.* **5**, 229 (1968)]. The NO-O_3 chemiluminescence technique was used to monitor both NO and O_3 [D. H. Stedman, E. E. Daby, F. Stuhl, H. Niki, *J. Air Pollut. Control Assoc.* **22**, 260 (1972)]. The NO_2 was monitored as NO after quantitative reduction (> 99 percent) by a Mo/C converter [L. P. Breitenbach and M. Shelef, *J. Air Pollut. Control Assoc.* **23**, 128 (1973)]. Other nitrogen-containing species, for example, NH_3 and HNO_3, did not significantly interfere with the NO_2-NO conversion, although they may cause a long-term drift in the base line.
14. The photolysis reaction is

$$HONO + h\nu \ (\lambda = 2900 \text{ to } 4000 \text{ Å}) \rightarrow HO + NO$$

where $h\nu$ is a phot H. S. Johnston and R. Graham, *Can. J. Chem.* **52**, 1415 (1974); R. A. Cox, *J. Photochem.* **3**, 175 (1974).

15. C. E. Junge, *Air Chemistry and Radioactivity*, vol. 4 of the International Geophysics Series, J. Mieghem, Ed. (Academic Press, New York, 1963).
16. E. Robinson and R. C. Robbins, *Stanford Res. Inst. Project PR-6755* (American Petroleum Institute, Washington, D.C., 1971).
17. W. Seiler, *Tellus* **26**, 116 (19 P. E. Wilkness, R. A. Lamontagne, R. E. Larson, J. W. Swimmerton, C. R. Dickson, T. Thompson, *Nature (Lond.)* **245**, 45 (1973).
18. D. H. Ehhalt, *Tellus* **26**, 58 (1974).
19. H. Levy, *Planet. Space Sci.* **20**, 919 (1972).
20. A major atmospheric source of HO involves the photolysis of O_3

$$O_3 + h\nu \ (\lambda < 3130 \text{ Å}) \rightarrow O(^1D) + O_2$$

followed by

$$O(^1D) + H_2O \rightarrow 2HO$$

21. The effect of a higher concentration of CO is to shift the ratio of $[HO_2]/[HO]$ to a higher value by the two reactions:

$$CO + HO \rightarrow CO_2 + H$$

and

$$H + O_2 + M \rightarrow HO_2 + M$$

followed by the decomposition of HO_2

$$2HO_2 \rightarrow H_2O_2 + O_2$$

The net effect is a reduced concentration of HO. At higher NO_2 concentrations, the reaction

$$HO + NO_2 + M \rightarrow HNO_3 + M$$

is a major removal mechanism of HO.

22. The formation of HONO in the atmosphere may occur according to the reactions

$$NO + NO_2 + H_2O \rightleftharpoons 2HONO$$

and

$$HO + NO + M \rightarrow HONO + M$$

23. P. A. Leighton, *Photochemistry of Air Pollution* (Academic Press, New York, 1961); H. S. Johnston, *Project Clean Air Document 7* (University of California, Berkeley, 1970).

6 May 1975

Epidermal Growth Factor: Identification of a New Hormone in Human Urine

Abstract. *Epidermal growth factor is a polypeptide hormone that was previously identified only in mice. It causes proliferation and keratinization of epidermal tissues. An immune affinity column extraction technique was used to purify partially a substance from human urine which was similar to the mouse hormone in both its biological activity and immunoreactivity.*

Epidermal growth factor (EGF) is a polypeptide hormone originally isolated from the submaxillary glands of adult male mice. Its discovery was a result of the observation that extracts of these glands caused precocious eye opening and tooth-bud eruption when injected into immature mice (*1*). These morphological effects are now known to be due to stimulation of epidermal growth and keratinization (*2*).

Since its discovery in 1962, considerable knowledge has accumulated about mouse EGF, much of which has been summarized (*3*). Mouse EGF is both heat and acid stable and has a molecular weight of 6045; its primary chemical structure is known (*4*). The metabolic events that occur when epidermal cells are exposed to EGF include stimulation of ornithine decarboxylase activity, accumulation of polyamines, and increased synthesis of RNA and protein (*5*). Initially, the biological assay for EGF was based on early eye opening in the immature mouse. Further elucidation of EGF physiology was made possible by the subsequent development of a sensitive and specific radioimmunoassay (*6*). In the mouse, submaxillary gland EGF concentration is dependent on androgen stimulation, but plasma EGF levels are not androgen dependent. Mouse urine, milk, and saliva contain much higher concentrations than does plasma. Alpha-adrenergic stimulation causes release of submaxillary gland EGF, resulting in marked increases in plasma EGF concentrations, and alpha-adrenergic blockade abolishes this response. Neither beta-adrenergic stimulation nor blockade has any effect. When the submaxillary glands are removed, the response of plasma EGF to alpha-adrenergic stimulation is abolished, yet basal plasma EGF concentrations are unchanged (*7*). This suggests that there may

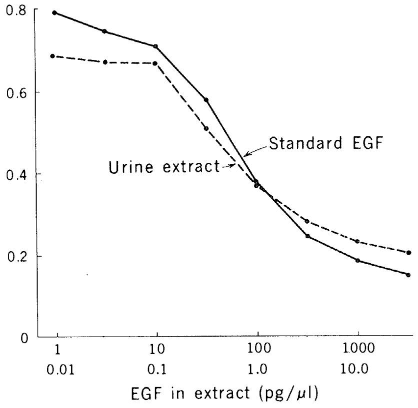

Fig. 1. Competitive binding curves of mouse EGF and affinity column extract of human urine. *B/F* is the ratio of antibody bound to free ^{125}I-labeled mouse EGF.